RESEARCH MEMORANDUM

DESIGN AND TEST OF MIXED-FLOW IMPELLERS

IV - EXPERIMENTAL RESULTS FOR IMPELLER MODELS MFI-1 AND MFI-2 WITH CHANGES IN BLADE HEIGHT

By Joseph T. Hamrick, William L. Beede,
and Joseph R. Withee, Jr.

Lewis Flight Propulsion Laboratory
Cleveland, Ohio

NATIONAL ADVISORY COMMITTEE
FOR AERONAUTICS

WASHINGTON
February 11, 1954

Classification cancelled (or changed to UNCLASSIFIED)

By authority of NASA Tech Pub Announcement #12
(OFFICER AUTHORIZED TO CHANGE)

By 10 Feb 58
NAME AND

GRADE OF OFFICER MAKING CHANGE

28 Mar 61
DATE

NATIONAL ADVISORY COMMITTEE FOR AERONAUTICS

RESEARCH MEMORANDUM

DESIGN AND TEST OF MIXED-FLOW IMPELLERS

IV - EXPERIMENTAL RESULTS FOR IMPELLER MODELS MFI-1 AND MFI-2 WITH CHANGES IN BLADE HEIGHT

By Joseph T. Hamrick, William L. Beede,
and Joseph R. Withee, Jr.

SUMMARY

Modifications A and B of impeller model MFI-1 and A, B, and C of impeller model MFI-2 were investigated experimentally in an attempt to determine what allowance in blade height should be made for boundary-layer and viscous losses in an impeller designed for isentropic compressible flow. A gradual increase in blade height was arbitrarily made from inlet to outlet in anticipation of a gradual build-up of boundary layer. Apparently there was a rapid build-up of boundary layer near the inlet in the experimental case rather than a gradual one. Therefore, the proper allowance for boundary layer cannot be prescribed from the data obtained.

Decreasing the pressure gradient along the shroud by reducing the blade height allowance apparently did little to increase the over-all efficiency. At the design speed of 1400 feet per second, the over-all adiabatic efficiency was increased from 0.83 for the MFI-1A to 0.85 for the MFI-1B with reduction in height; however, it is indicated from the theoretical velocity distribution and outlet surveys that the increase was due to a change from decelerating to accelerating flow along the hub rather than from any change along the shroud. It is further indicated that the consequences of a thickened or separated boundary layer depend not only on the design velocity gradients but also on the shape of the passage.

INTRODUCTION

A series of mixed-flow centrifugal impellers is being designed and experimentally investigated at the NACA Lewis laboratory, in order to develop a reliable aerodynamic design procedure that will reduce or eliminate the large amount of aerodynamic development work necessary in the past. For the first two models of this series, impeller models

MFI-1 and MFI-2 of references 1 to 3, which were designed for isentropic compressible flow, the blade height was arbitrarily increased by an amount varying gradually from zero at inlet to 74 percent of the outlet radial blade height at outlet. The purpose of the increase was to allow for a gradual build-up of boundary layer as well as to increase the ratio of blade height to passage width. The amount of increase was made greater than was considered necessary in order to allow for reduction in several steps to the blade height for isentropic flow.

The region of greatest boundary-layer build-up will probably occur along the impeller shroud where the maximum decrease in velocity from inlet to outlet must take place. With the present limited knowledge of the boundary-layer behavior in a rotating passage and enclosing shroud, the maximum allowable velocity gradients for which boundary-layer separation may be avoided cannot easily be determined. Although there has been excellent progress in the study of turbulent boundary layer and separation in recent years (refs. 4 to 8), it is difficult to apply the results of these studies to centrifugal compressors. The effect on the flow movement relative to the shroud and the secondary-flow effects within the passage, such as those discussed in reference 9, are among factors that are difficult to evaluate in making application of known theory.

An attempt is made in this investigation to provide an analysis of the results obtained with changing blade height that will aid the designer in making allowance for viscous effects. The procurement of experimental data that afford a precise evaluation of the results is very difficult, inasmuch as measurements within the rotating passage are required. In this investigation the instrumentation of the impeller to obtain measurements in the rotating passages was considered impracticable; therefore, an approximate evaluation is presented that is based on total-pressure surveys just downstream of the impeller exit, static-pressure measurements on the stationary shroud, and over-all performance. The over-all performance characteristics of two versions of the MFI-1 impeller and three versions of the MFI-2 impeller are presented.

SYMBOLS

The following symbols are used in this report:

f_s slip factor, ratio of absolute tangential velocity at exit to impeller speed at exit, taken herein as ratio of over-all enthalpy rise to $\dfrac{\left(\begin{array}{c}\text{impeller-outlet speed at root-mean-square} \\ \text{radius from hub to shroud}\end{array}\right)^2}{gJ}$

L ratio of distance from impeller inlet measured along surface of shroud to total length of shroud

P_0 stagnation pressure upstream of inlet

p static pressure

Q ratio of velocity relative to impeller to speed of sound for inlet stagnation conditions

U actual impeller speed based on 7.00-in. radius, ft/sec

W actual air weight flow, lb/sec

δ ratio of inlet total pressure to NACA standard sea-level pressure (29.92 in. Hg abs)

η_{ad} adiabatic temperature-rise efficiency

θ ratio of inlet total temperature to NACA standard sea-level temperature (518.4° R)

APPARATUS, INSTRUMENTATION, AND PROCEDURE

Apparatus

Except for the change in shroud and outer-diffuser-wall dimensions, the apparatus is the same as that for the MFI-1A in reference 2. Two impellers, the MFI-1 and the MFI-2, which have different hub and blade shapes but identical inlet and outlet annuli and shroud shapes, were used in the investigation. In the first step, the basic blade height (for isentropic flow) was increased by an amount varying from zero at inlet to 74 percent of the outlet radial blade height at outlet. In the second step, the increase was reduced by half. In the third step, which was omitted for the MFI-1, the allowance was eliminated. The impeller designations for steps one, two, and three, respectively, are the MFI-1A and MFI-2A (configuration A), the MFI-1B and MFI-2B (configuration B), and the MFI-2C (configuration C). Photographs of the MFI-1A and MFI-2A and the shroud shapes for the three configurations are shown in figure 1. The shroud dimensions for configuration A are the same as those for the MFI-1A and MFI-2A of references 1 to 3; and for configuration C, the same as those for the MFI-1 and MFI-2 impellers of references 1 to 3. The shroud dimensions for configuration B were determined by taking the average of the shroud radii for configurations A and C at each axial depth. The outer diffuser wall for configuration C was designed to give constant diffuser area from inlet to outlet. For configuration B, the outer-diffuser-wall radii were determined by taking the average of the outer-diffuser-wall radii for configurations A and C in the first inch of diffuser length of configuration A with constant area thereafter.

The splitter vanes shown in figures 1(a) and (c) were an arbitrary addition to the MFI-1A and MFI-1B only, and were not a part of the isentropic design.

Instrumentation

Except for outlet surveys, the instrumentation is the same as that described in reference 2. All surveys from hub to shroud were made at an average distance of approximately 7/8 inch from the impeller exit at the survey station shown in figure 1 at equivalent speeds of 1400 feet per second. For the MFI-1A, a three-hole 1/4-inch-diameter cylindrical yaw tube was used. It was found that for angle measurements the claw-type probe (fig. 2) was more accurate on the basis of integrated values of weight flow at the survey station; therefore, the claw-type probe was used for the MFI-1B. For surveys at the exits of the three versions of the MFI-2, for which low-temperature air was used at the speed of 1400 feet per second, pressure fluctuations in the air supply made rapid measurements desirable; therefore, a shielded total-pressure probe similar to that shown in reference 9 was used. A comparison of total-pressure surveys with the shielded and the claw probes showed only small differences (1 percent at mid-passage to 4 percent near walls); and, because of angle insensitivity up to $\pm 40^{\circ}$ with the shielded probe, the surveys could be made rapidly where flow-angle measurements were not desired.

3136

Procedure

The procedure for determination of over-all performance and slip factor based on measurements at the over-all measuring station is the same as that for reference 2. In computing velocity at the survey station, only wall static pressures were used. A straight-line variation in static pressure from the inner to the outer wall was assumed. Low-temperature air was used at the speed of 1600 feet per second for the MFI-1 and at 1300 and 1400 feet per second for the MFI-2, in order to reduce the actual speed as a safety precaution. The mean line of 7 inches was used in setting the impeller speed for all blade heights. Therefore, the actual tip speed decreased with decreasing blade height.

ACCURACY OF SURVEYS

Values of integrated weight flow based on measurements at the survey station with the three-hole cylindrical yaw tube were of the order of 40 percent too high as compared with measurements with a submerged adjustable orifice. It was thought that the large size of the probe (0.250-in. diam.) in comparison with the passage height (0.6 in.)

contributed to large errors in angle measurements. In the neighborhood of the flow angle at the survey station for the outlet mean-line speed of 1400 feet per second, an error of 1° in flow angle produced an error of approximately 4 percent in weight flow. With the claw-type probe of figure 2, the integrated weight flow varied from 17 percent too high for the weight flow of 13 pounds per second to 13 percent too high at the weight flow of 14 pounds per second. It is probable that fluctuations in the absolute velocity, which may be large (as shown in ref. 9), caused errors in both the pressure and angle measurements. As pointed out on page 47 of reference 10, the manometer reading will be too high for total-pressure measurements in a pulsating stream. Although the measured total pressure will be only a small percentage too high (variations of ±20 percent give a reading only 2 percent too high), the error in angle measurement may be large because of a fluctuating flow angle.

Although there is some doubt about the absolute accuracy of the surveys, variations in errors (from one blade height to the next), caused by flow fluctuations, are probably much smaller than the measured pressure differences, and the repeatability of the data indicates that any mechanical error is consistent. Therefore, the total-pressure profiles are considered adequate for comparison from one impeller blade height to the next.

EXPERIMENTAL RESULTS

Impeller Model MFI-1

Over-all performance. - The over-all performance characteristics for the MFI-1A and the MFI-1B are given in figure 3. Over-all pressure ratio is plotted against weight flow for the range of speeds with constant efficiency contours superimposed in figures 3(a) and (b), and over-all efficiency is plotted against weight flow for the range of speeds in figures 3(c) and (d). A comparison of peak pressure ratio, maximum efficiency, slip factor, and weight-flow range is shown in figure 4. The pressure ratio for the MFI-1A, even though it has a generally lower efficiency, is approximately the same as that for the MFI-1B because of the higher tip speed for the MFI-1A. The slip factor (fig. 4) for the MFI-1B should be lower than for the MFI-1A because of the backward blade curvature at outlet. With backward blade curvatures, the higher relative through-flow velocity results in a higher negative tangential component of relative velocity for the lower blade height. At the lower impeller-outlet speeds where this component of velocity is larger in proportion to the impeller speed, the decrease in slip factor is more in evidence. The difference in maximum weight flow (fig. 4) decreases from minimum speed to maximum speed as the choke point moves from the impeller outlet toward the impeller inlet where the blade height is the same for the two impellers. The surge weight flow for the MFI-1B, except at the outlet speed of 700 feet per second, is lower than for the MFI-1A.

Static pressure. - The experimental static-pressure distribution along the shroud for the MFI-1A and MFI-1B is compared with the theoretical distribution for the MFI-1 in figure 5. The MFI-1 has the basic blade height and no splitter vanes. The assumption of perfect guidance of the fluid by the impeller blades and the difficulty in obtaining an accurate solution in mixed supersonic and subsonic flow regions as discussed in reference 2 are probably responsible for the disagreement of theoretical and experimental data near the inlet. The maintenance of a more nearly constant difference between the experimental and theoretical values for the lower blade height suggests a rapid build-up of boundary layer near the inlet rather than the gradual build-up along the shroud for which the increase in blade height was made.

Outlet surveys. - The ratio of total pressure across the passage at the survey station to inlet stagnation pressure is given in figure 6 for the MFI-1A and MFI-1B. The gradient in energy input across the passage based on constant slip factor is such that, for the MFI-1B, the pressure ratio at the 80-percent distance across the passage (fig. 6) would be approximately 5.0 if the efficiency there equaled that at the 20-percent distance; therefore, a thick boundary layer is indicated near the shroud for both the MFI-1A and MFI-1B.

Impeller Model MFI-2

Over-all performance. - The over-all performance characteristics for the MFI-2A, MFI-2B, and MFI-2C are given in figure 7. Over-all pressure ratio is plotted against weight flow for the range of speeds, with constant efficiency contours superimposed, in figures 7(a) to (c); and over-all efficiency is plotted against weight flow for the range of speeds in figures 7(d) to (f). A comparison of peak pressure ratio, maximum efficiency, slip factor, and weight-flow range is shown in figure 8. There was no increase in efficiency with reduction in blade height as there was with the MFI-1 in going from configuration A to B. There was a large increase in slip factor in going from configuration A to C. It was pointed out in reference 3 that separation off the trailing face could be the reason that the slip factor is lower than the design value of 1.00. Another factor that might be responsible may be explained as follows: There is no change in angular momentum with increasing impeller radius for that portion of the fluid that is uninfluenced by the blades near the outlet. Therefore, in order for the blade to unload and at the same time to maintain the tangential velocity of the fluid equal to that of the blade at outlet, it was necessary for the tangential component of absolute velocity of the fluid upstream of the outlet to be greater than that at the outlet. This was brought about by forward blade curvature just upstream of the outlet. For example, on the mean line the

design absolute tangential component of velocity of the fluid at the 6-inch radius is 1460 feet per second as compared with the impeller-outlet mean-line speed of 1400 feet per second. With the increase in blade height, the relative velocity (and thus the tangential component upstream of the outlet) probably fell below the design value and reduced the slip factor. As with the MFI-1, the maximum-weight-flow plot (fig. 8) indicates movement of the choke point from the inlet toward the outlet with reduction in impeller speed. For outlet speeds below 1300 feet per second, the surge weight flow is reduced with reduction in blade height.

Static pressure. - The experimental static-pressure distribution along the shroud for the MFI-2A, MFI-2B, and MFI-2C is compared with the theoretical distribution for the MFI-2C in figure 9. The leveling off of static pressure and departure from the theoretical distribution for the MFI-2A at a distance ratio L of 0.30 may indicate separation along the shroud, inasmuch as the leveling-off point moves to L of 0.37 in the MFI-2B and to 0.57 in the MFI-2C. The leveling off at L = 0.25 for the MFI-2C is peculiar, in that it does not appear with the MFI-2A and MFI-2B. As with the MFI-1, the maintenance of a more nearly constant difference between the experimental and theoretical values for the lowest blade height suggests a rapid build-up of boundary layer near the inlet. Because of the higher blade height in the MFI-2, the reduction in height makes less change in the through-flow area of the MFI-2 than for the MFI-1 (except at the outlet) and therefore a smaller change in the static pressure along the shroud.

Outlet surveys. - The ratio of total pressure across the passage at the survey station to inlet stagnation pressure is given in figure 10 for the MFI-2A, MFI-2B, and MFI-2C. The change in profile is somewhat less than that for the MFI-1 with reduction in blade height.

DISCUSSION OF RESULTS

Efficiency

The MFI-1A impeller has an efficiency 4 points higher than the MFI-2A at mean-line speed of 1400 feet per second (0.83 compared with 0.79). With the first reduction in blade height to configuration B, the difference became 6 points, with a 2-point improvement in efficiency for the MFI-1 (0.85) and none for the MFI-2. Further reduction in blade height resulted in reduced efficiency for the MFI-2C to 0.77.

Except for leveling out of the static pressure along the shroud where separation may have occurred for the MFI-2A, the static-pressure distributions on the shroud (figs. 5 and 9) and the outlet-survey profiles of the MFI-1A and MFI-2A (figs. 6 and 10) are similar. If

separation did occur in the MFI-2, it perhaps accounts for a large part of the difference in efficiency between the MFI-1 and MFI-2.

With the reduction in blade height to the MFI-1B and MFI-2B, there was a much larger change in the total-pressure-ratio profile at outlet for the MFI-1 (fig. 6) than for the MFI-2 (fig. 10). The following explanation of this occurrence is based on a study of the theoretical relative velocity distribution along the hub and the through-flow component of velocity for the MFI-1A at the survey station. The theoretical average velocity between blades along the hub of the MFI-1 and MFI-2C is given in figure 11 for a weight flow of 13 pounds per second and an outlet mean-line speed of 1400 feet per second. From an L ratio of 0.8 to the outlet, there is a large deceleration for the MFI-2C, but not for the MFI-1. In view of this, it is probable in the experimental case that there is a change from decelerating flow along the hub near the outlet in the MFI-1A to accelerating average flow in the MFI-1B, and decelerating flow at all blade heights in the MFI-2. Accelerating flow on the hub would tend to prevent the build-up of boundary layer and bring about the improvement in total-pressure profile from the MFI-1A to the MFI-1B shown in figure 6. Thus, it appears that there is considerable merit in designing for continuous acceleration of the average flow from inlet to outlet on the hub.

3136

Separation

In the investigations of reference 9, there was little indication of flow separation within the rotating passage. Instead, the air of low kinetic energy appeared to have moved to the blade trailing face at the hub and to have accumulated at a point on the shroud approximately 80 percent of the passage width from the driving (pressure) face. The static-pressure variation from inlet to outlet indicated that this secondary-flow movement took place smoothly with no abrupt changes in pressure such as that indicated for the MFI-2 in figure 9; therefore, it is conjectured that separation did occur in the MFI-2 along the shroud.

There is a slight change in direction for the static-pressure distribution along the shroud of the MFI-1B in figure 5; but, from the shape of the curve for the MFI-1A and comparison with the theoretical curve, if separation did occur it was not of sufficient proportion to cause sudden blockage of the flow. Inasmuch as the static-pressure gradients along the shroud are similar for the two impellers (MFI-1 and MFI-2) and the over-all gradient for the MFI-2B is not as severe as that for the MFI-1A, it appears that pressure gradients (or velocity gradients) are not the controlling factor as regards separation in this case. With the rapid build-up of boundary layer in the passage as is indicated by the static-pressure profile, perhaps in the MFI-1, which has relatively low blade height compared with the MFI-2, the boundary layer extends from

shroud to hub, and separation is rendered unstable by a large attendant increase in free-stream velocity just downstream of the separation point. If this is the case, design of the hub-shroud profile based on the principle of the divergent diffusers (refs. 11 and 12) may be desirable.

It was suggested in reference 3 that separation along the trailing face at exit may have caused a reduction in slip factor for the MFI-2A because of the large backward curvature of the blade at the driving face. In light of the results of reference 9, an accumulation of low-energy air at the trailing face adjacent to the hub could have produced a similar result without separation. The increases in total-pressure ratio near the inner wall for the MFI-1B (fig. 6) and the MFI-2B (fig. 10) (as compared with the MFI-1A and MFI-2A, respectively), which were accompanied by an increase in slip factor for both impellers at the outlet speed of 1400 feet per second, indicate that this may be the case.

Allowance for Viscous Effects

In the computations of reference 2, a value of 0.90 was assumed for internal relative efficiency, and it was indicated that at outlet the experimental relative velocity and static pressure for the MFI-1A were approximately equal to that for isentropic design with no increase in blade height. It is indicated from the through-flow component of average velocity at the survey station for the MFI-1B that except at the hub the experimental outlet relative velocity even for the MFI-1B is lower than the theoretical value for the MFI-1. Thus, it appears that the assumed relative efficiency of 0.90 in reference 2 was too high; and, with respect to velocity, the allowance for boundary layer at the outlet was too great for both the MFI-1A and MFI-1B.

With respect to decreases in static pressure due to viscous losses and boundary-layer blockage, the blade-height increase near the outlet of the MFI-1A appears to be approximately correct. However, as has been pointed out, the boundary layer apparently builds up rapidly near the inlet, and sufficient allowance was not made except near the outlet. The foregoing discussion applys also to the MFI-2.

General Considerations

The results obtained in this investigation cannot be used to determine directly the magnitude or location of a boundary-layer allowance. Further, what may be an allowable pressure or velocity gradient along the shroud for one impeller configuration may not be satisfactory for another configuration. These considerations suggest that, for the large deceleration that must take place along the shroud of this type impeller, the passage shape and not the velocity gradient may be the primary factor.

For example, cutting down the MFI-2 tended to move the apparent separation point toward the outlet along the shroud at the expense of a higher Mach number at the outlet, but did not eliminate separation. Thus, the efficiency was not increased, but even decreased, in going to the lowest blade height.

The increase in efficiency for the MFI-1 in going from the MFI-1A to the MFI-1B apparently was not the result of any change along the shroud, but of a change in boundary-layer profile along the hub. Judging from the theoretical results and the outlet surveys (fig. 6), there probably was a change in this case from an average deceleration to acceleration along the hub. Apparently the accelerating flow tended to reduce the boundary layer at the hub and thus reduce the accumulation of low-energy air along the trailing face as discussed in reference 9.

There are at least three distinct sources of loss associated with boundary-layer build-up along the hub and shroud within the rotating passage. First, there is the build-up of boundary layer on the shroud that may give rise to secondary-flow movements of low-energy air toward the trailing face. This low-energy air may be met by low-energy air moving from the trailing face because of leakage through the hub-to-shroud clearance space and possibly form a vortex on the shroud, as discussed in reference 9. Second, there is separation of the boundary layer on the shroud; and third, there is build-up of boundary layer on the hub with accumulation of low-energy air adjacent to the trailing face due to secondary flow (ref. 9).

Apparently, separation was prevented on the shroud of the MFI-1 but not in the MFI-2, which may account for a large part of the difference in efficiency for the two impellers. In addition, the third source of loss was greatly reduced in the MFI-1B. It appears, therefore, that of the three sources of loss mentioned, the only one that is very difficult to eliminate is that associated with boundary-layer build-up and secondary flow on the shroud.

SUMMARY OF RESULTS

Two impellers, the MFI-1 and the MFI-2, were investigated experimentally in an attempt to determine the allowance in blade height that should be made for boundary-layer and viscous losses in an impeller designed for isentropic compressible flow. In the first step (impellers MFI-1A and MFI-2A), an allowance was made in which the basic blade height was increased from zero at inlet to 74 percent of the outlet radial blade height at outlet. The gradual increase was made in expectation of a gradual build-up of boundary layer. In the second step (impellers MFI-1B and MFI-2B), the allowance was reduced by half. In the third step (impeller MFI-2C), which was omitted for the MFI-1, the allowance was eliminated. The following results were obtained:

1. The maximum over-all adiabatic efficiency of the MFI-1A (step one) at the design speed of 1400 feet per second was 0.83 and of the MFI-1B (step two) was 0.85.

The maximum over-all efficiency of the MFI-2A (step one) at the design speed of 1400 feet per second was 0.79; of the MFI-2B, 0.79 (step two); and of the MFI-2C, 0.77 (step three).

2. The boundary layer appears to build up rapidly near the inlet of the impeller, not gradually as was expected. Therefore, the prescription of an increase in blade height to allow for boundary-layer and viscous losses cannot be made from the data obtained.

3. It is indicated that the consequences of a thickened or separated boundary layer depend not only on the design velocity gradients but also on the shape of the passage. Changing the deceleration rate on the shroud by reducing the blade height apparently did little to increase the over-all efficiency. It is indicated from the theoretical velocity distribution and the outlet surveys that the increase in efficiency from the MFI-1A to the MFI-1B was due to a change from decelerating to accelerating flow along the hub rather than from any change along the shroud.

Lewis Flight Propulsion Laboratory
National Advisory Committee for Aeronautics
Cleveland, Ohio, November 27, 1953

REFERENCES

1. Osborn, Walter M., and Hamrick, Joseph T.: Design and Test of Mixed-Flow Impellers. I - Aerodynamic Design Procedure. NACA RM E52E05, 1952.

2. Withee, Joseph R., Jr., and Beede, William L.: Design and Test of Mixed-Flow Impellers. II - Experimental Results, Impeller Model MFI-1A. NACA RM E52E22, 1952.

3. Hamrick, Joseph T., Osborn, Walter M., and Beede, William L.: Design and Test of Mixed-Flow Impellers. III - Design and Experimental Results for Impeller Model MFI-2A and Comparison with Impeller Model MFI-1A. NACA RM E52L22a, 1953.

4. Von Doenhoff, Albert E., and Tetervin, Neal: Determination of General Relations for the Behavior of Turbulent Boundary Layers. NACA Rep. 772, 1943. (Supersedes NACA WR L-382.)

5. Garner, H. C.: The Development of Turbulent Boundary Layers. R. & M. No. 2133, British A.R.C., June 1944.

6. Ludwieg, H., and Tillmann, W.: Investigations of the Wall-Shearing Stress in Turbulent Boundary Layers. NACA TM 1285, 1950.

7. Maskell, E. C.: Approximate Calculation of the Turbulent Boundary Layer in Two-Dimensional Incompressible Flow. Rep. No. AERO. 2443, British R.A.E., Nov. 1951.

8. Bagley, J. A.: The Prediction of Boundary Layer Separation on the Approach Surfaces of Two-Dimensional Air Intakes in Incompressible Flow. Rep. No. AERO. 2173, British R.A.E., June 1952.

9. Hamrick, Joseph T., Mizisin, John, and Michel, Donald J.: Study of Three-Dimensional Internal Flow Distribution Based on Measurements in a 48-Inch Radial-Inlet Centrifugal Impeller. NACA TN 3101, 1954.

10. Prandtl, L., and Tietjens, O. G.: Applied Hydro- and Aeromechanics. McGraw-Hill Book Co., Inc., 1934.

11. Young, A. D., and Green, G. L.: Tests of High-Speed Flow in Diffusers of Rectangular Cross-Section. R. & M. No. 2201, British A.R.C., July 1944.

12. Vedernikoff, A. N.: An Experimental Investigation of the Flow of Air in a Flat Broadening Channel. NACA TM 1059, 1944.

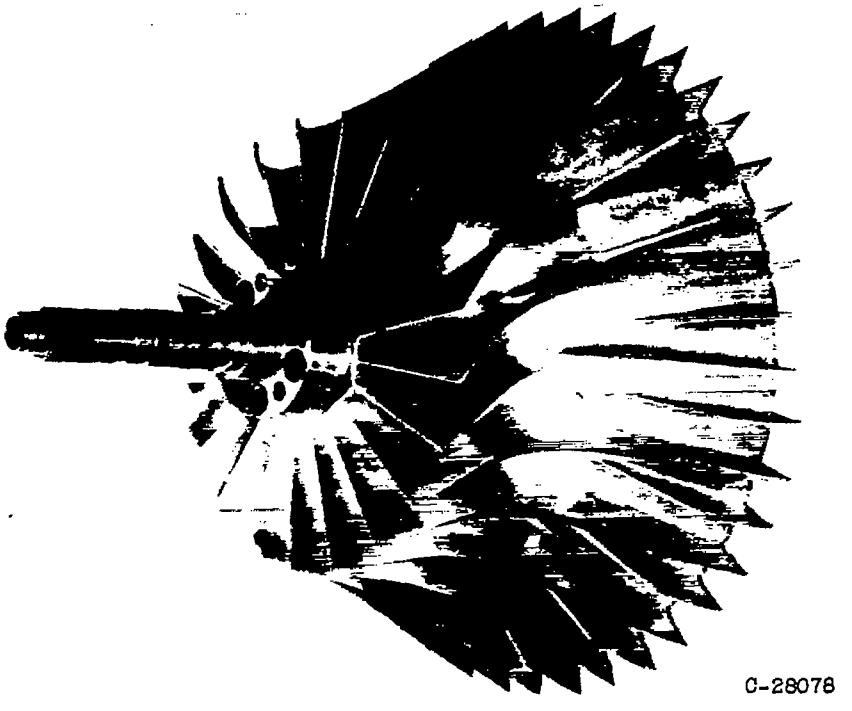

C-28078

(a) MFI-1A.

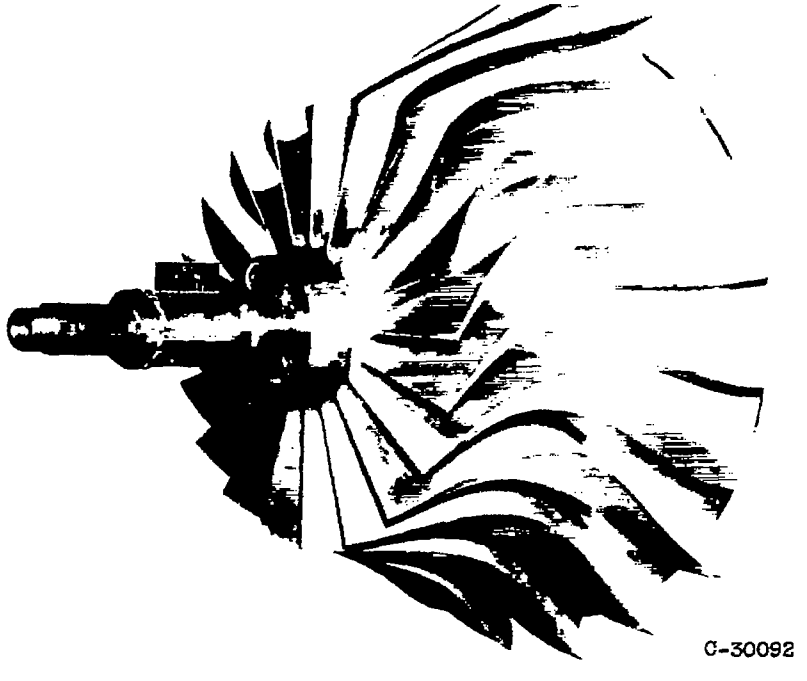

C-30092

(b) MFI-2A.

Figure 1. - Impeller shapes.

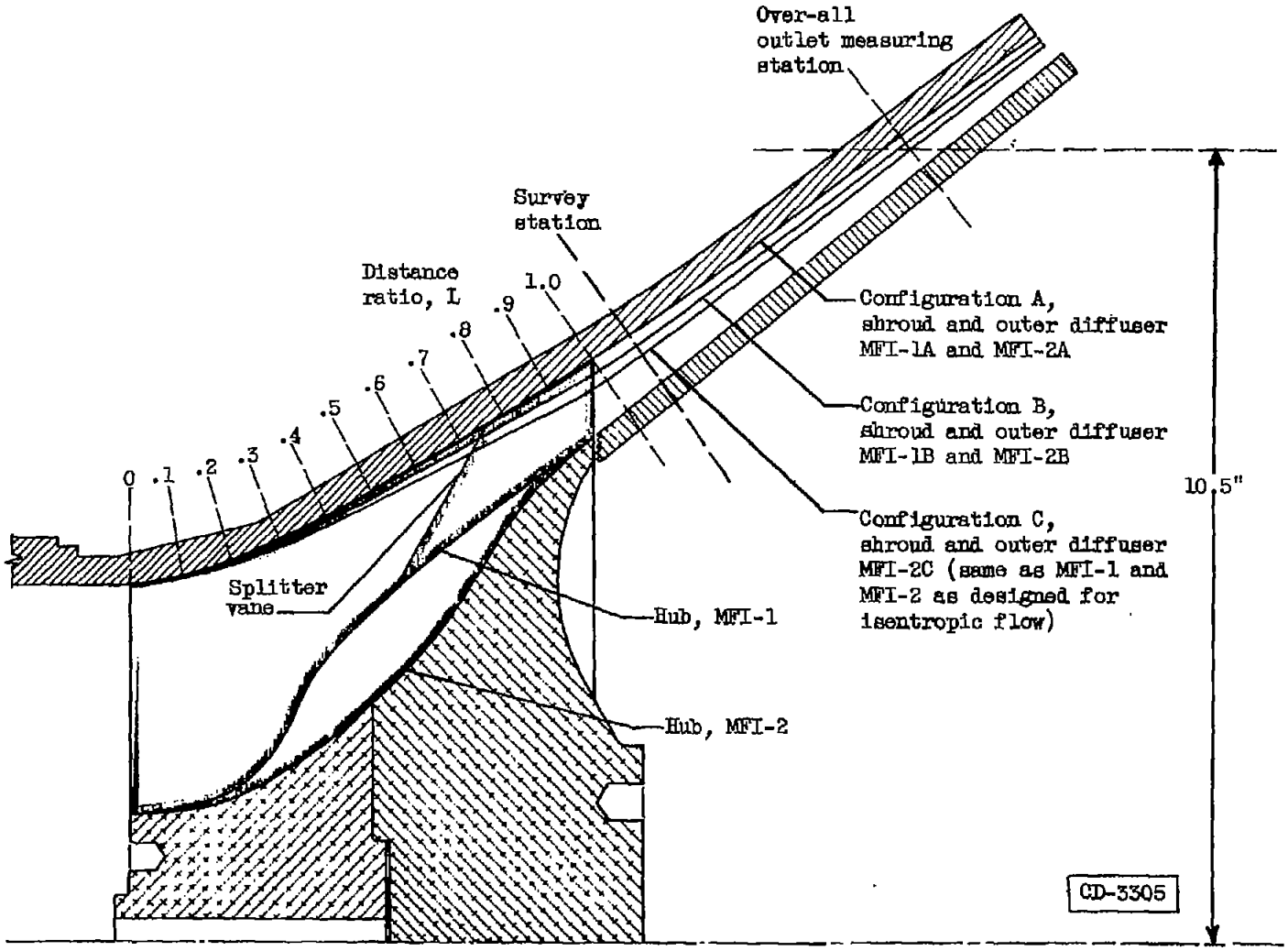

(c) Cross-sectional view showing variation in passage height.

Figure 1. - Concluded. Impeller shapes.

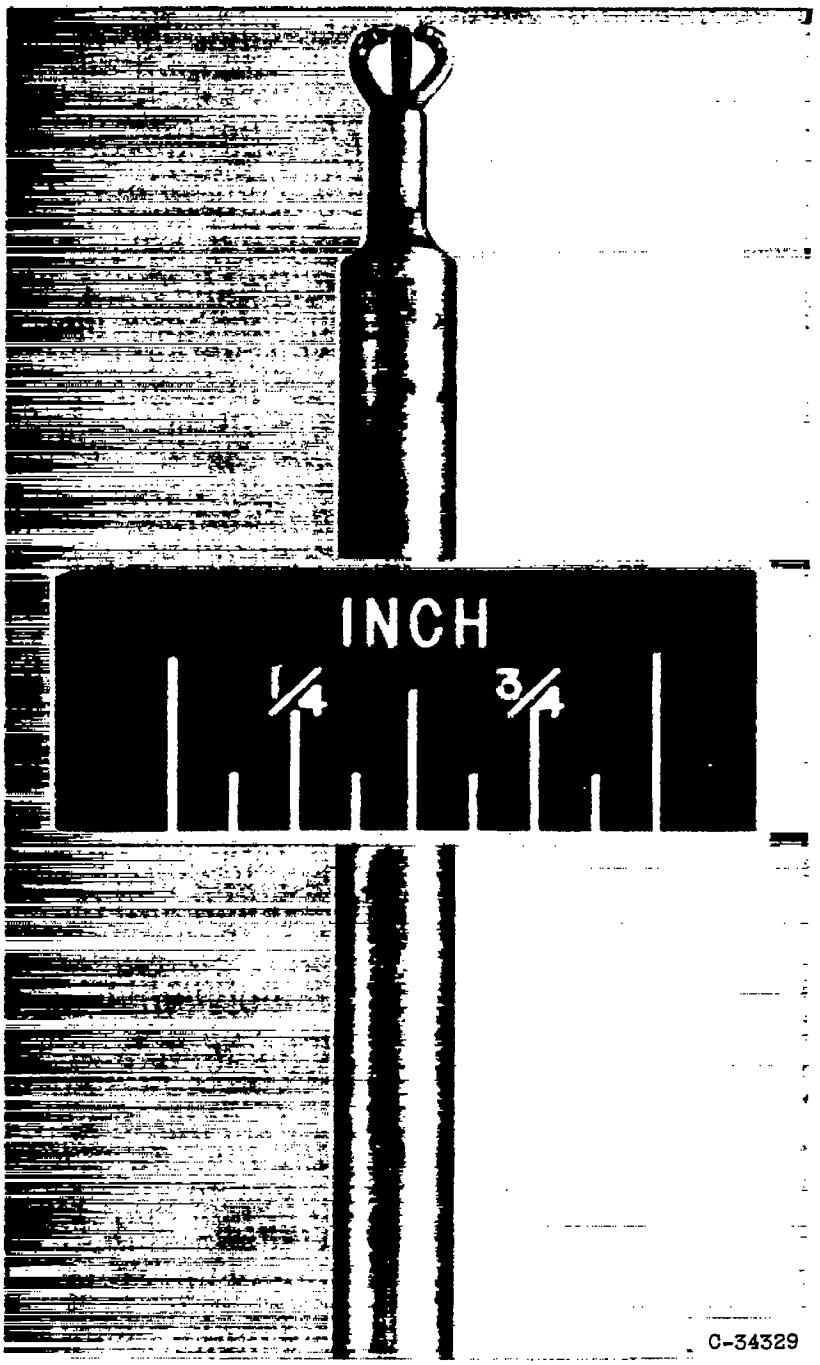

Figure 2. - Claw-type probe.

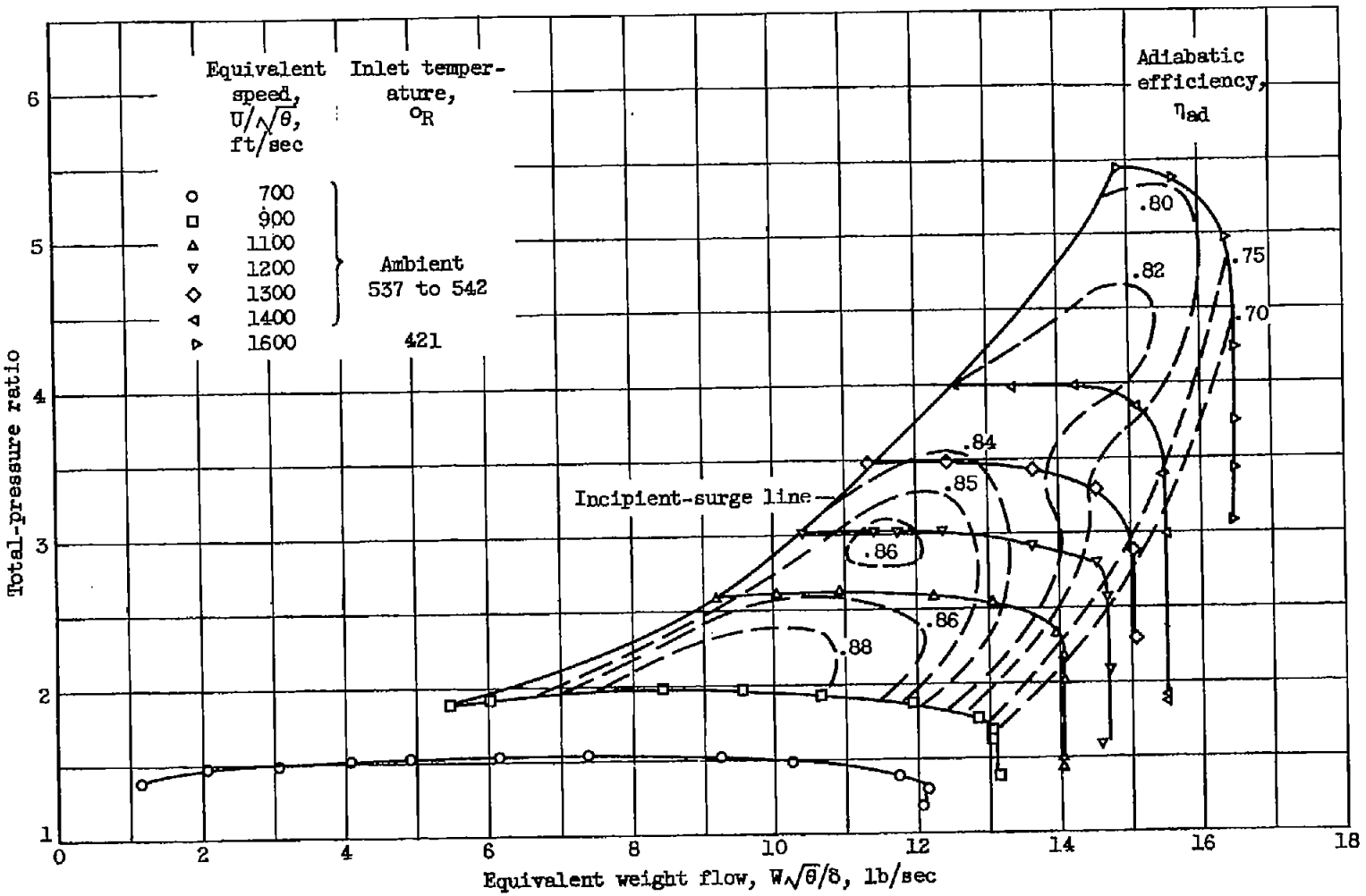

(a) Performance characteristics, MFI-1A.

Figure 3. - Over-all performance characteristics of MFI-1 impeller at inlet-air pressure of 14 inches of mercury absolute.

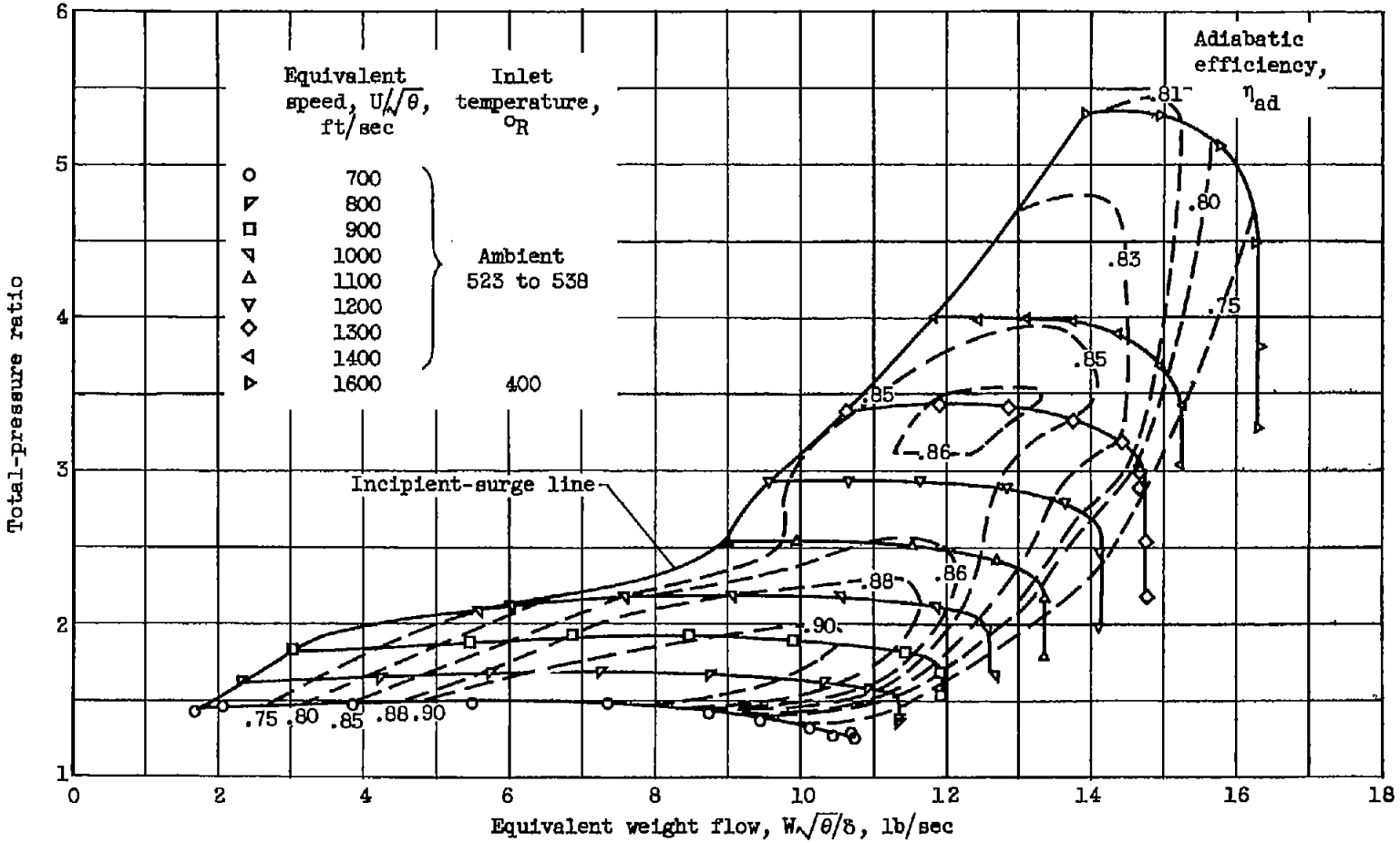

(b) Performance characteristics, MFI-1B.

Figure 3. - Continued. Over-all performance characteristics of MFI-1 impeller at inlet-air pressure of 14 inches of mercury absolute.

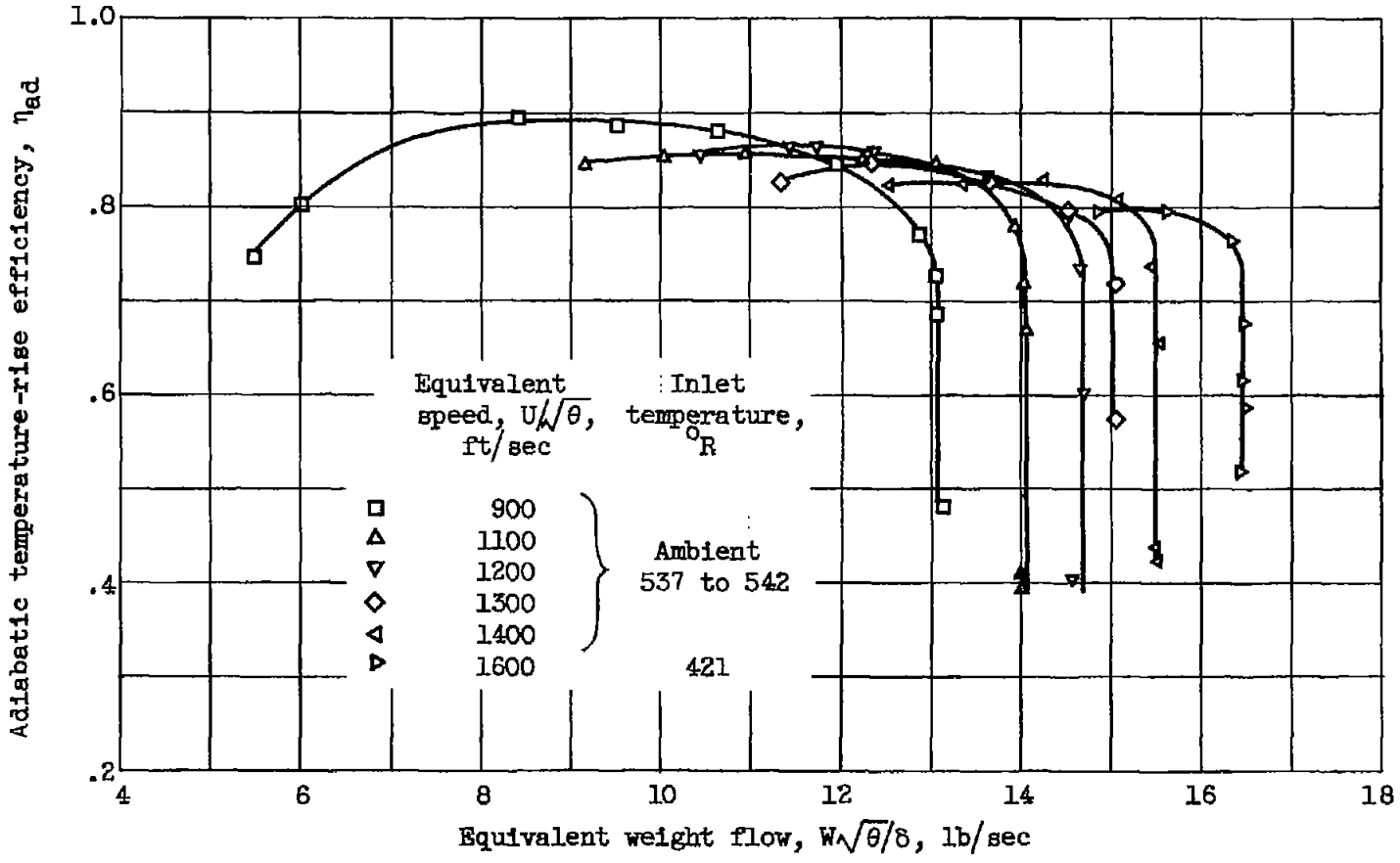

(c) Over-all efficiency, MFI-1A.

Figure 3. - Continued. Over-all performance characteristics of MFI-1 impeller at inlet-air pressure of 14 inches of mercury absolute.

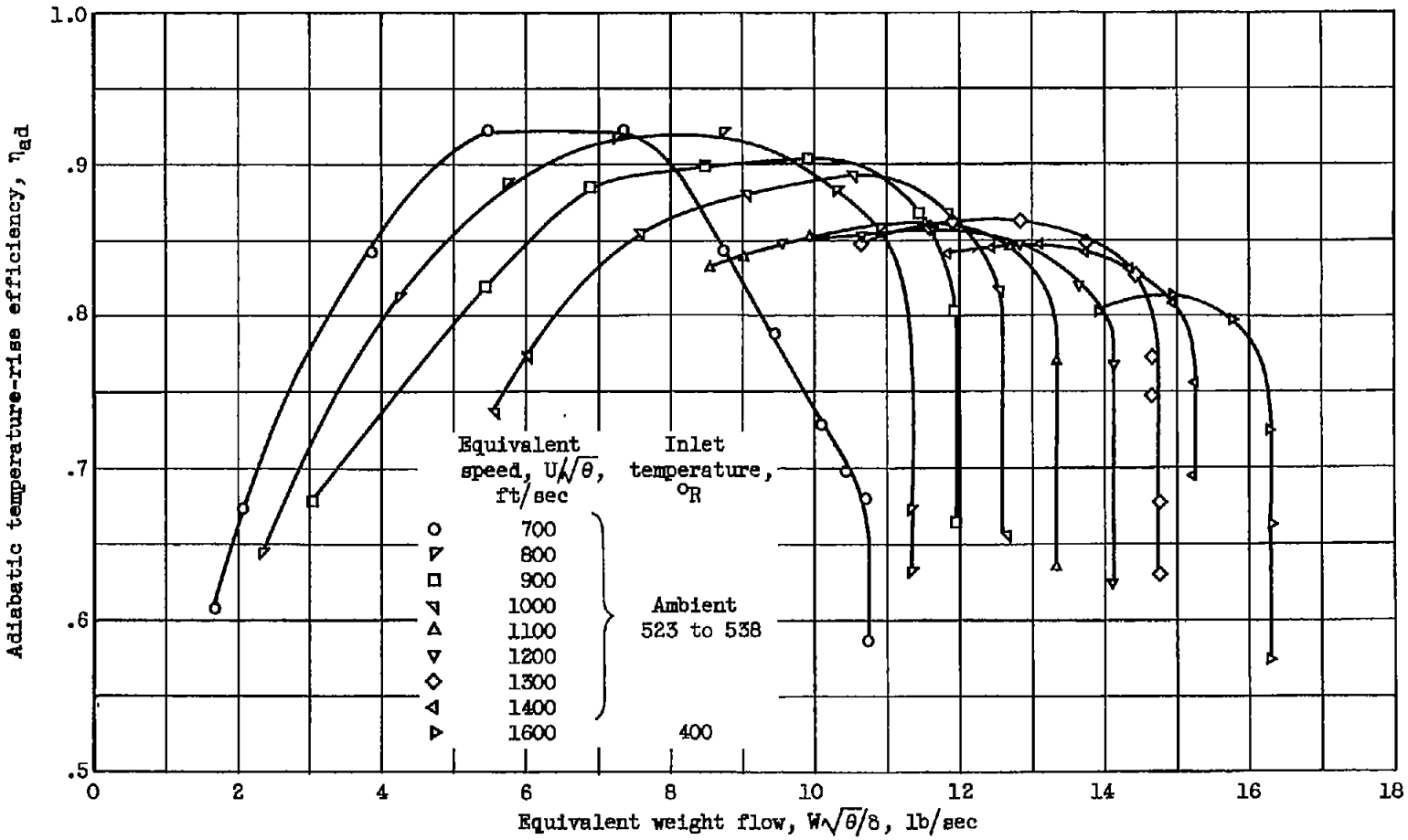

(d) Over-all efficiency, MFI-1B.

Figure 3. - Concluded. Over-all performance characteristics of MFI-1 impeller at inlet-air pressure of 14 inches of mercury absolute.

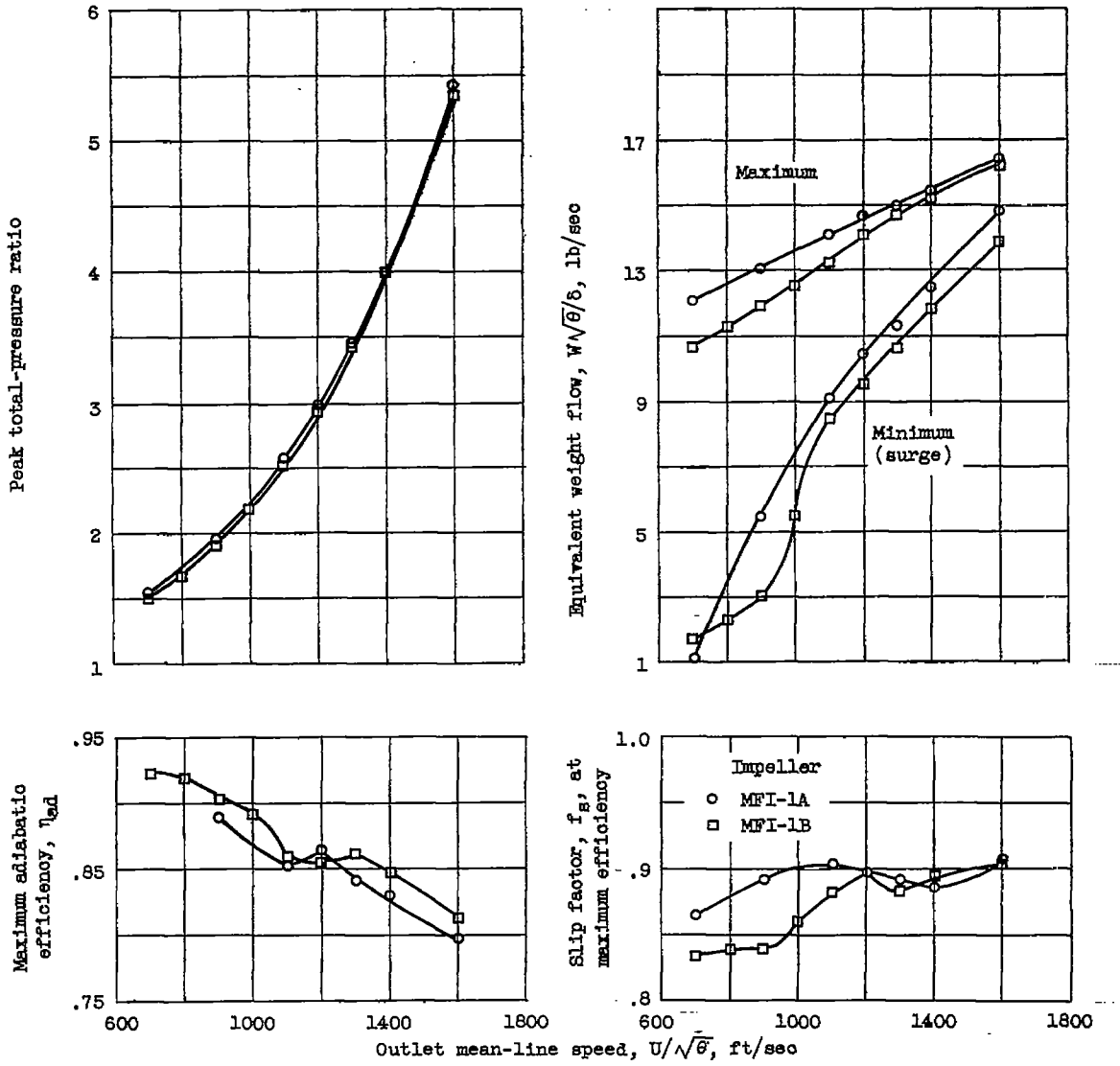

Figure 4. - Comparison of performance of impellers MFI-1A and MFI-1B.

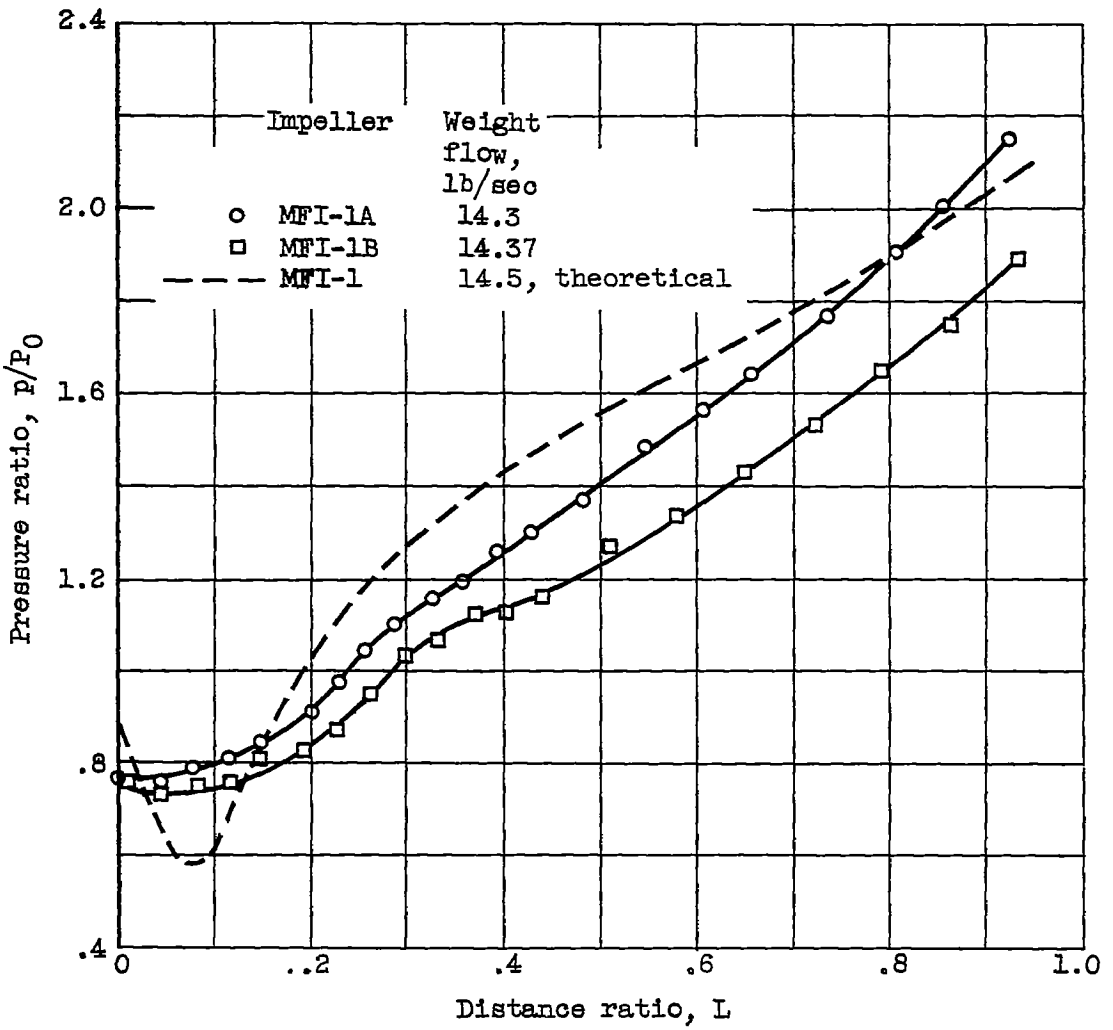

Figure 5. - Comparison of static pressures along shrouds of MFI-1A and MFI-1B. Outlet mean-line speed, 1400 feet per second.

[redacted]

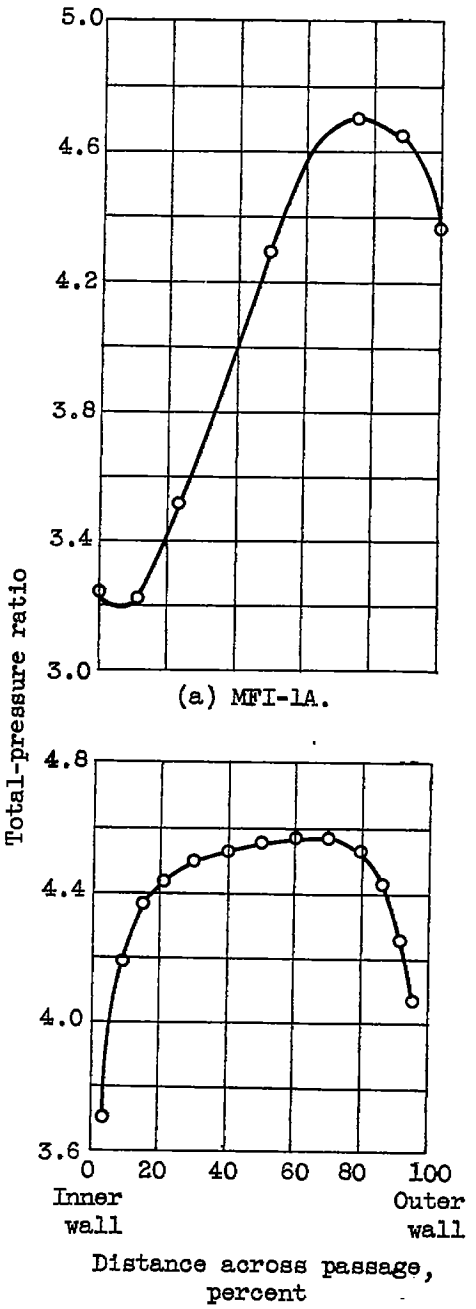

(a) MFI-1A.

(b) MFI-1B.

Figure 6. - Outlet total-pressure surveys for MFI-1A and MFI-1B. (Location of survey station shown in fig. 1.) Outlet mean-line speed, 1400 feet per second; equivalent weight flow, 13.5 pounds per second.

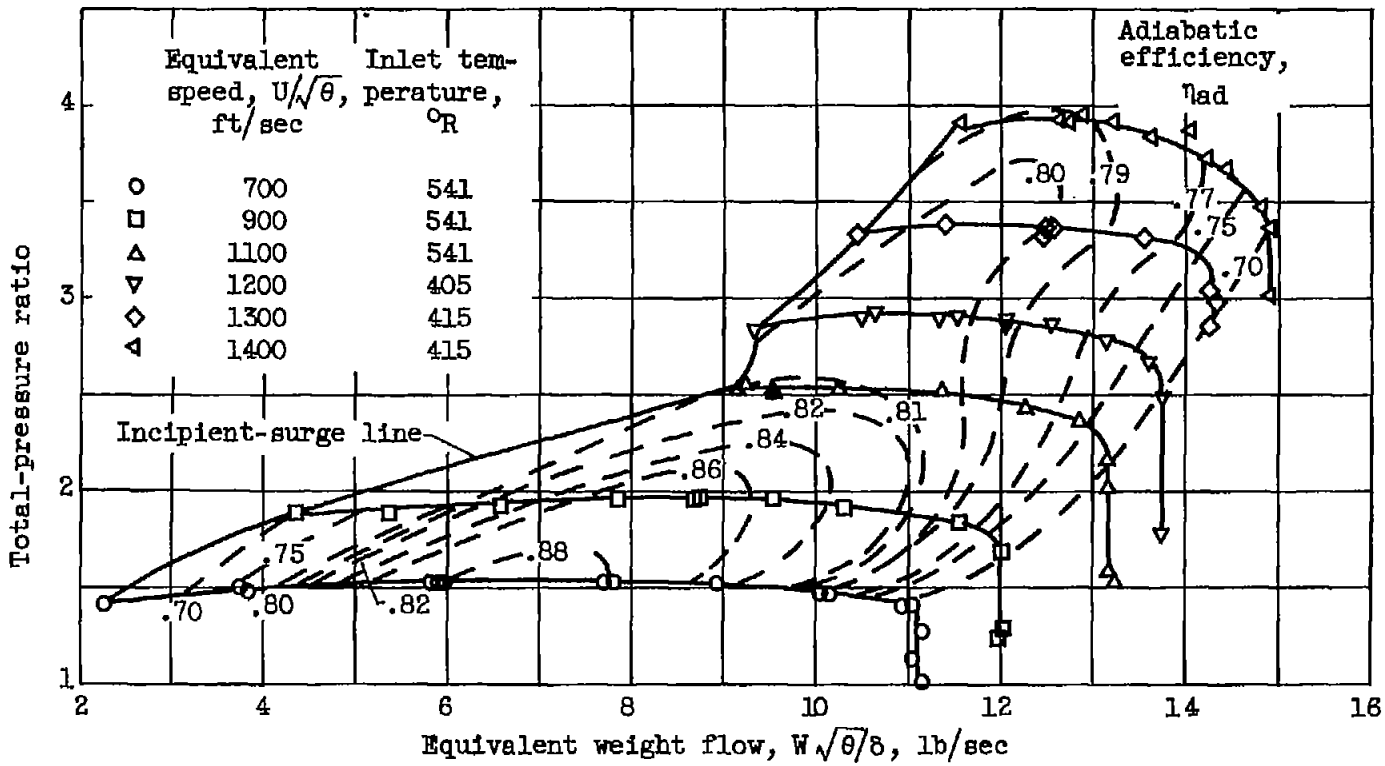

(a) Performance characteristics, MFI-2A.

Figure 7. - Over-all performance characteristics of MFI-2 impeller at inlet-air pressure of 14 inches of mercury absolute.

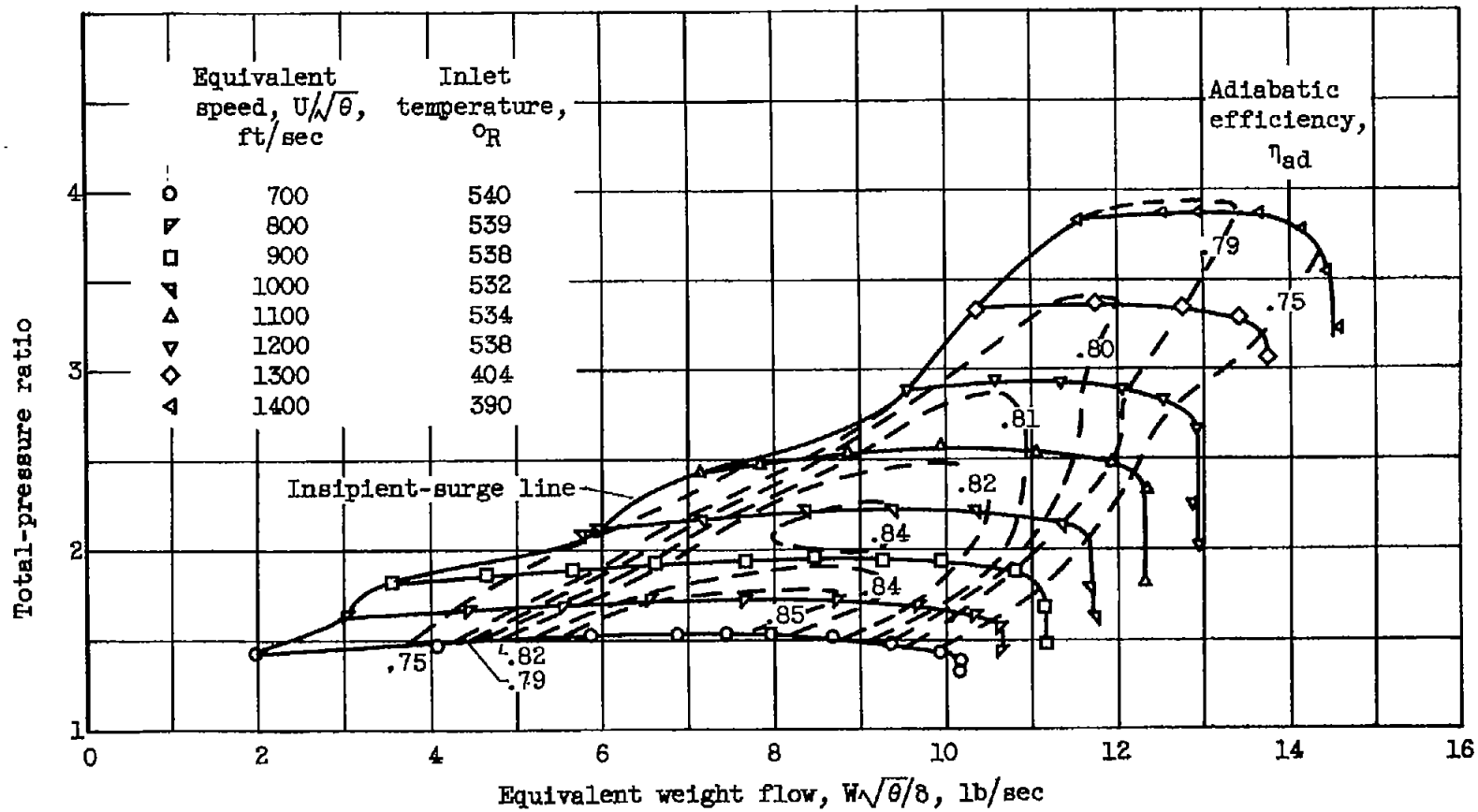

(b) Performance characteristics, MFI-2B.

Figure 7. - Continued. Over-all performance characteristics of MFI-2 impeller at inlet-air pressure of 14 inches of mercury absolute.

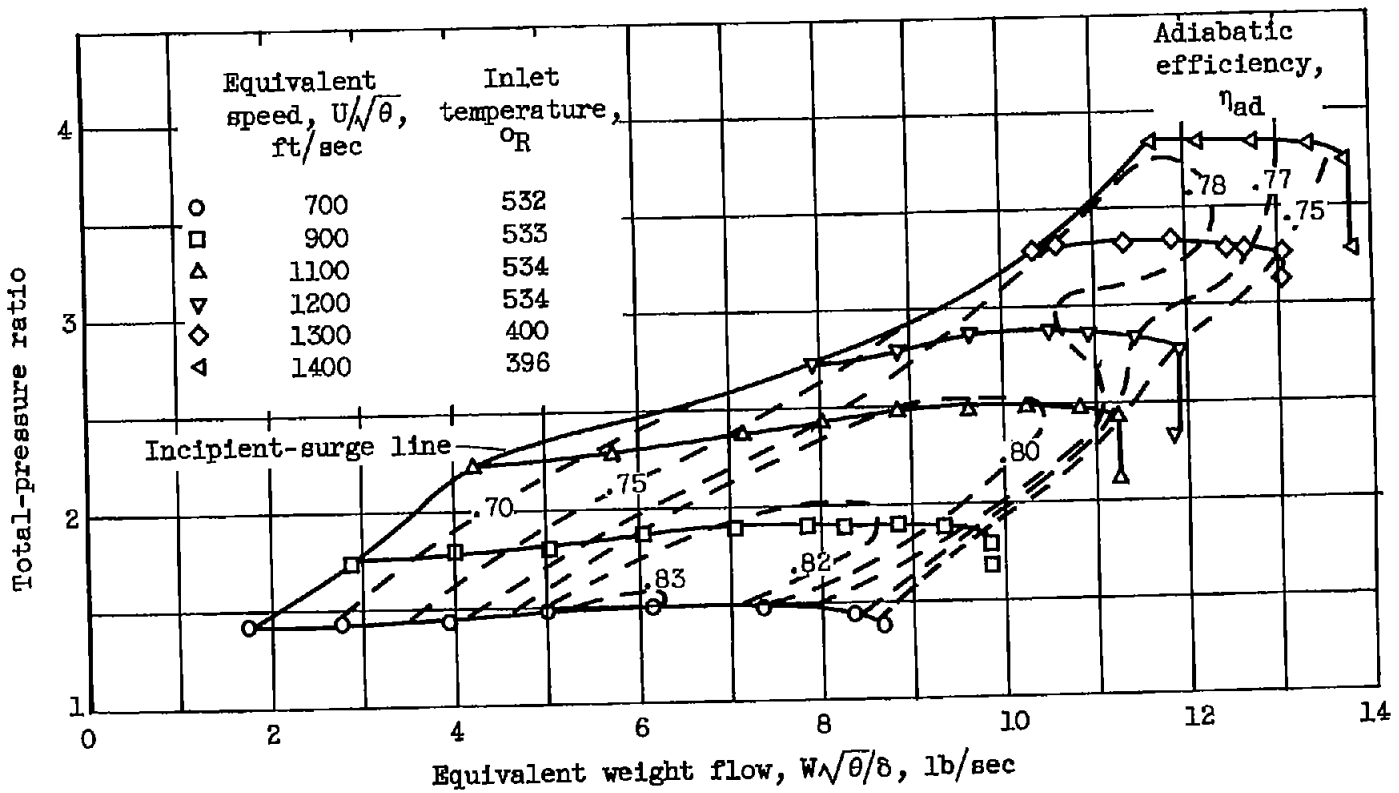

(c) Performance characteristics, MFI-2C.

Figure 7. - Continued. Over-all performance characteristics of MFI-2 impeller at inlet-air pressure of 14 inches of mercury absolute.

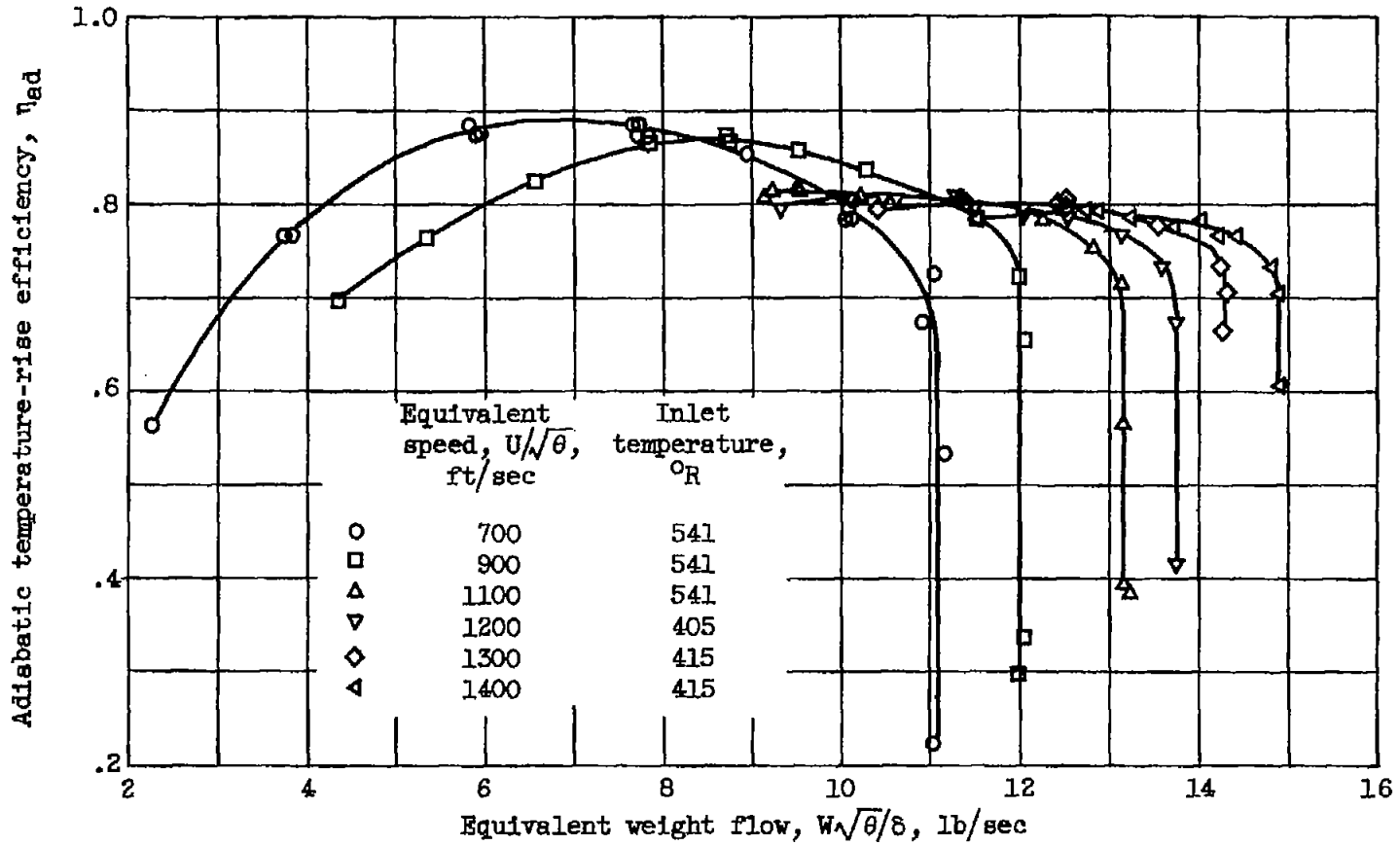

(d) Over-all efficiency, MFI-2A.

Figure 7. - Continued. Over-all performance characteristics of MFI-2 impeller at inlet-air pressure of 14 inches of mercury absolute.

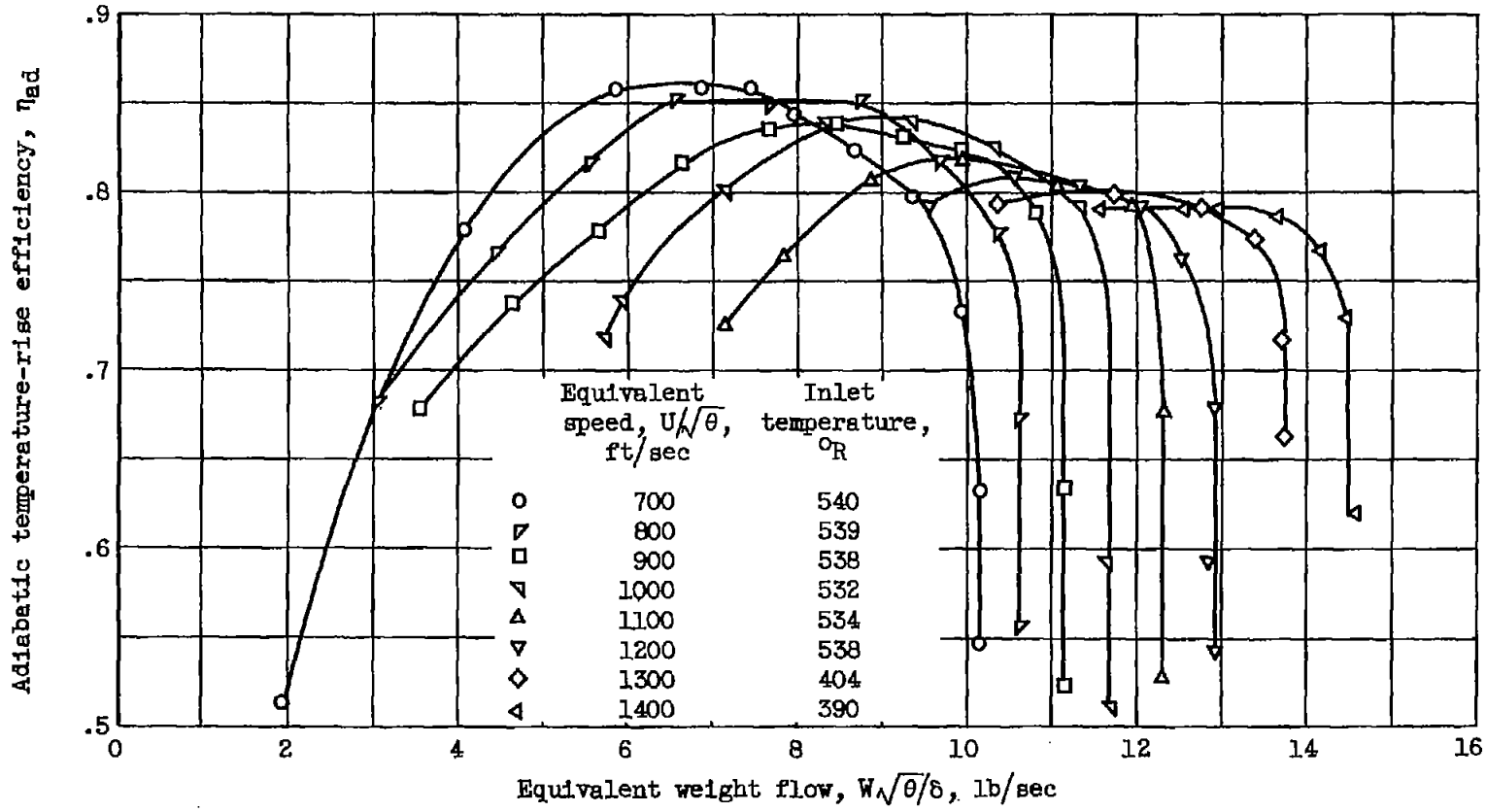

(e) Over-all efficiency, MFI-2B.

Figure 7. - Continued. Over-all performance characteristics of MFI-2 impeller at inlet-air pressure of 14 inches of mercury absolute.

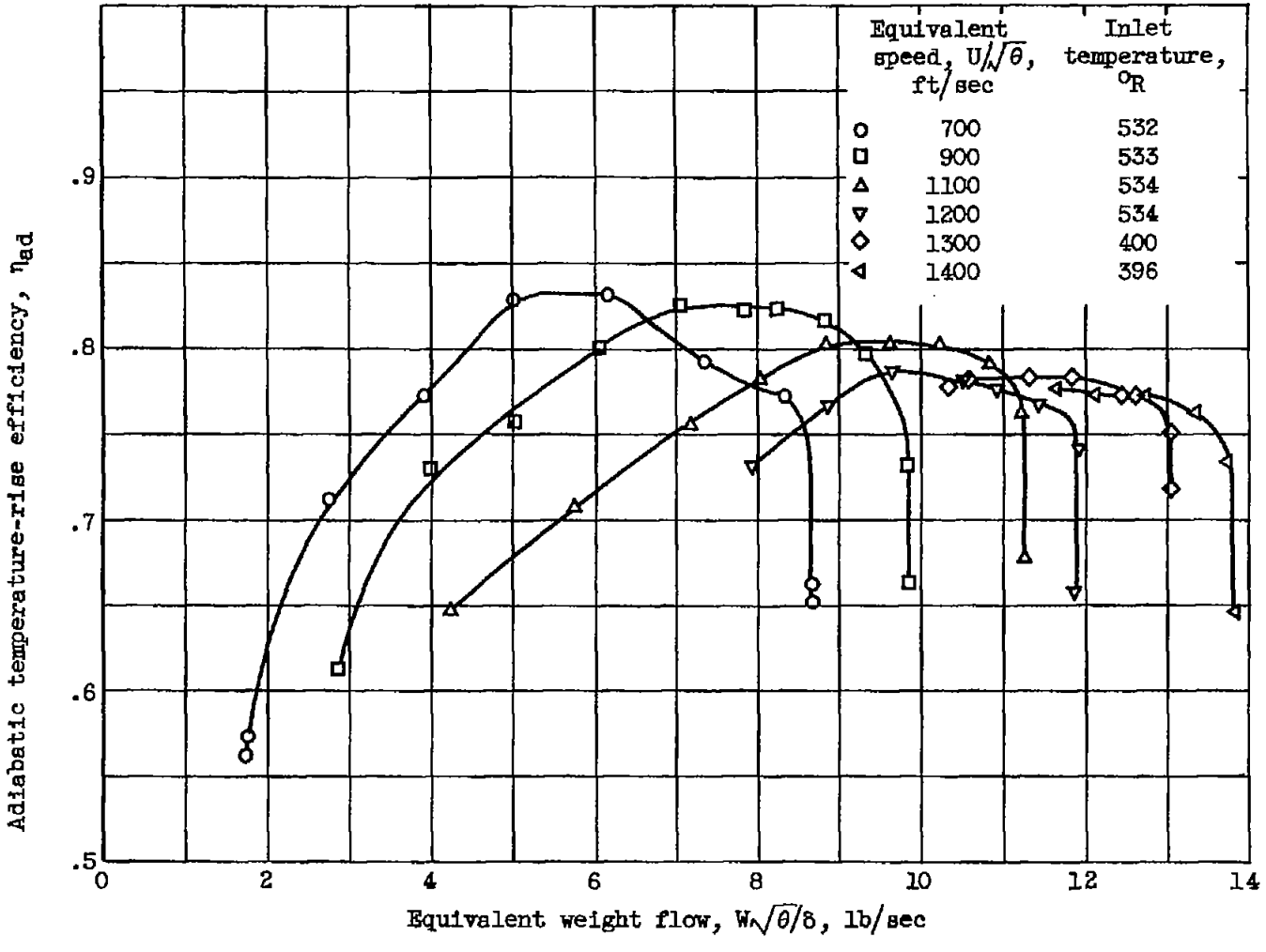

(f) Over-all efficiency, MFI-2C.

Figure 7. - Concluded. Over-all performance characteristics of MFI-2 impeller at inlet-air pressure of 14 inches of mercury absolute.

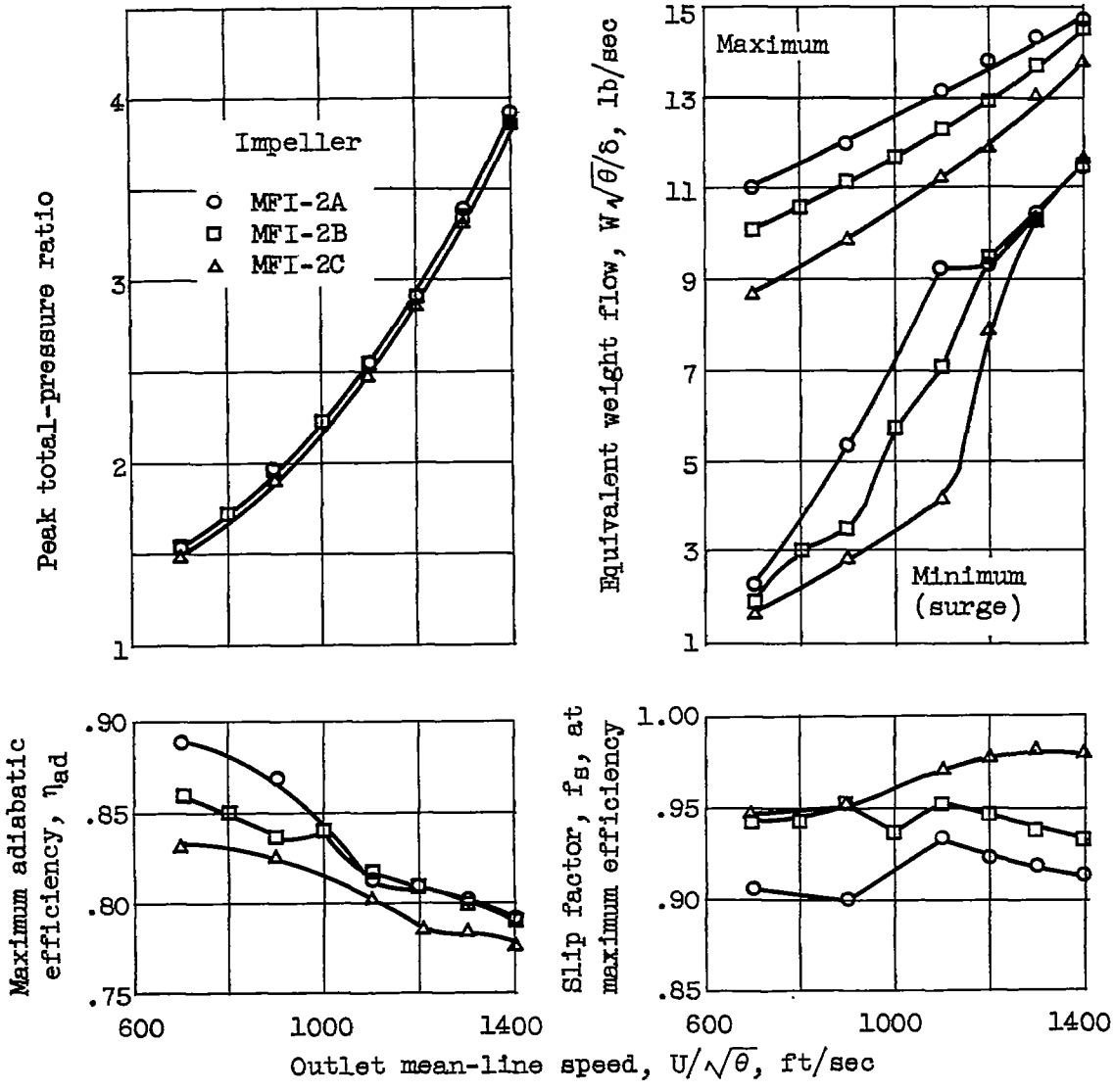

Figure 8. - Comparison of performance of impellers MFI-2A, MFI-2B, and MFI-2C.

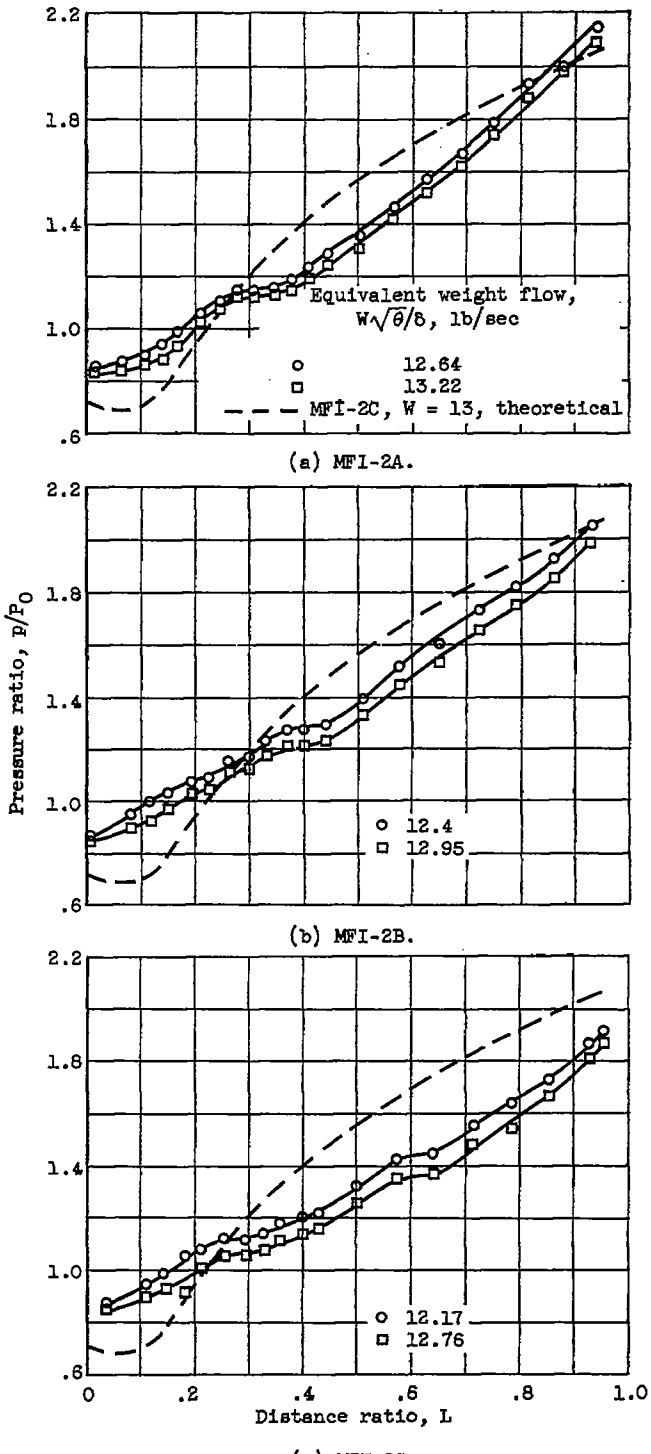

Figure 9. - Static-pressure ratios along shroud of MFI-2 for outlet speed of 1400 feet per second.

CONFIDENTIAL

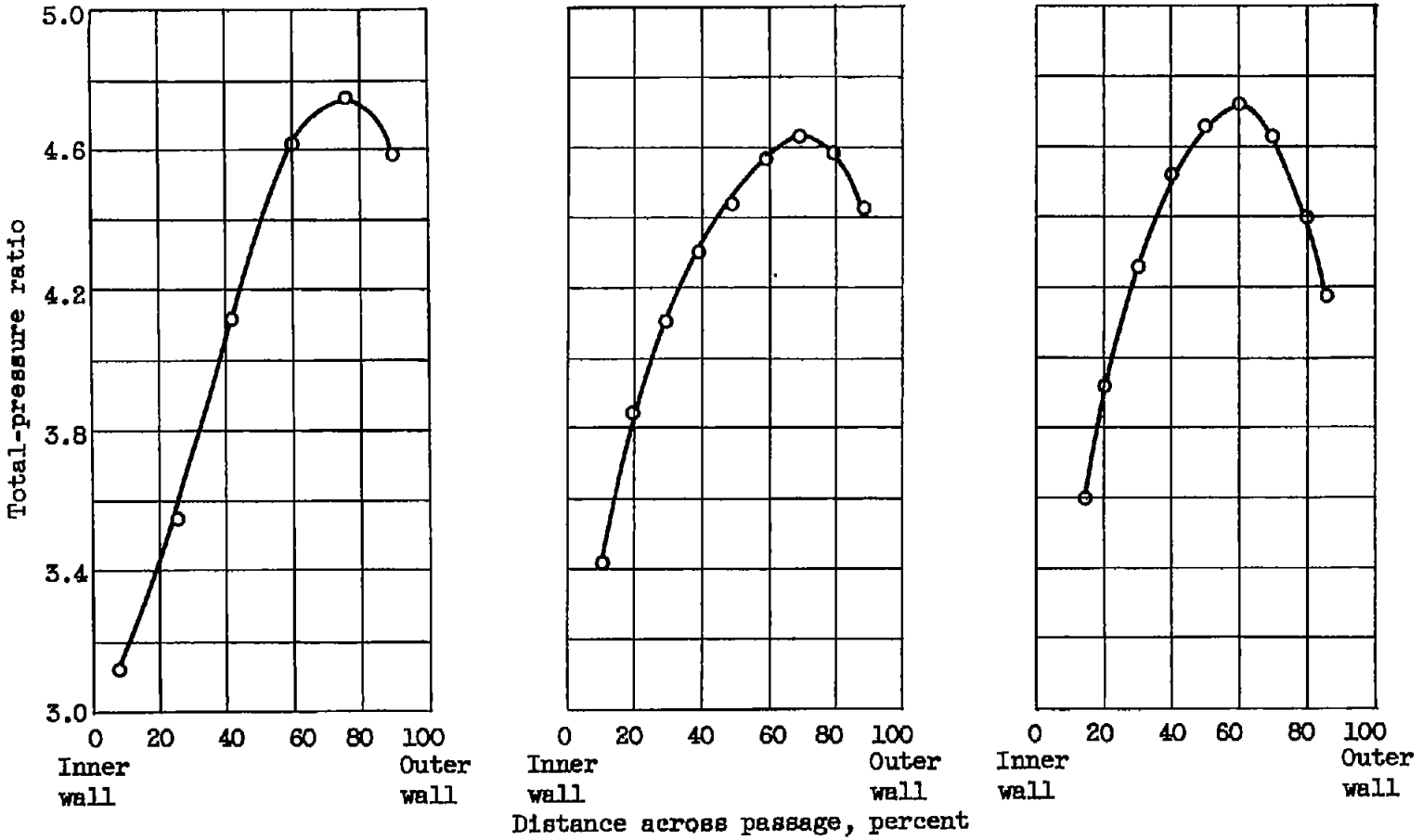

(a) MFI-2A. (b) MFI-2B. (c) MFI-2C.

Figure 10. - Outlet total-pressure surveys for MFI-2A, MFI-2B, and MFI-2C. (Location of survey station shown in fig. 1.) Outlet mean-line speed, 1400 feet per second; equivalent weight flow, 13.0 pounds per second.

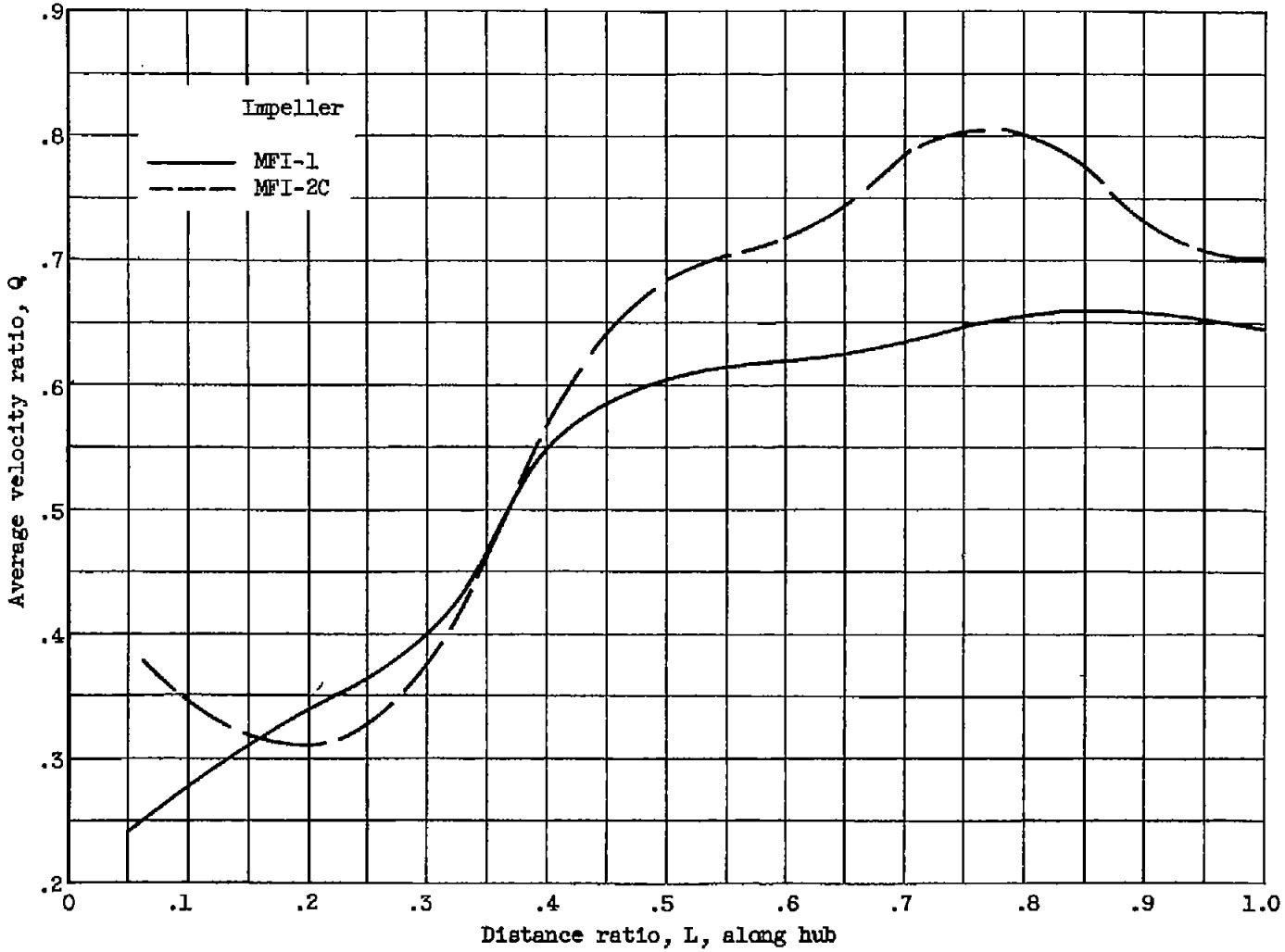

Figure 11. - Comparison of theoretical average velocity along hub for MFI-1 and MFI-2C. Outlet mean-line speed, 1400 feet per second; weight flow, 13.0 pounds per second.